Among the evaluation criteria for determining the efficiency of vehicle windshield cleaning, the pressure distribution of the wiper rubber brush on the glass surface is important. The problem is the lack of this indicator standardization by the United Nations Economic Commission for Europe Rules (UNECE) regarding the windshield wipers certification. The inhomogeneity of the pressure distribution of the conventional wiper (the object of research) is additionally due to the mobility of the links of its mechanism and the plasticity of the rubber brush together with the blade. The pressure value should not be more than 30–50 kPa (33.4 kPa was recorded for the immobilized wiper case), and the external normal load on the frame should be kept within 20…30 N. Under a load of 24 N, the wiper blade was deformed by 1.48 mm (according to R43, it cannot exceed 1.5 mm). Further loading of the wiper frame causes two types of plastic deformation: local and global (loss of the rubber brush shape). Local displacements have increased to 1.82 mm, and the shape of the blade has acquired a "sliced" character, which causes thin jets of dirt. Global ones led to the rubber brush bending with the gap between it and the glass (5.7 mm) and caused the blind zone appearance. Models to mathematically predict layer-by-layer deformations of a conventional wiper were investigated. A model of a double-row blade with separate brushes was built, which enables the parallelization of water flows and explains the increase in the efficiency of its design. Hydrodynamic tests showed 1.58 times greater effectiveness compared to a classic single-row blade: the water flow rate was 15.61 vs 9.86 m/s. This technological advancement is the subject of a patent and a possible working prototype

Keywords: distributed pressure, plastic deformations, stressed-strained state, damping, hydrodynamics, volume flow rate, turbulence

UDC 629.113
DOI: 10.15587/1729-4061.2024.298204

DETERMINING THE CHARACTERISTICS OF CONTACT INTERACTION BETWEEN THE TWO-ROW WINDSHIELD WIPER AND A CURVILINEAR GLASS SURFACE

Kostyantyn Holenko
PhD, Senior Lecturer*
Aleksandr Dykha
Corresponding author
Doctor of Technical Sciences, Professor, Head of Department*
E-mail: tribosenator@gmail.com
Yurii Voichyshyn
Postgraduate Student***
Orest Horbay
Doctor of Technical Sciences, Professor***
Maksym Dykha
PhD, Senior Lecturer
Department of Automation, Computer-Integrated Technologies and Robotics**
Volodymyr Dytyniuk
PhD, Lecturer*
*Department of Tribology, Automobiles and Materials Science**
**Khmelnytskyi National University
Instytuts'ka str., 11, Khmelnytskyi, Ukraine, 29016
***Department of Equipment Design and Operation
Lviv Polytechnic National University
S. Bandery str., 12, Lviv, Ukraine, 79013

Received date 15.11.2023
Accepted date 01.02.2024
Published date 28.02.2024

How to Cite: *Holenko, K., Dykha, A., Voichyshyn, Y., Horbay, O., Dykha, M., Dytyniuk, V. (2024). Determining the characteristics of contact interaction between the two-row windshield wiper and a curvilinear glass surface. Eastern-European Journal of Enterprise Technologies, 1 (7 (127)), 48–59. doi: https://doi.org/10.15587/1729-4061.2024.298204*

1. Introduction

Normative requirements for windshield wipers are regulated by a number of international rules, in particular the United Nations Economic Commission for Europe (UNECE) in the European Union and the Federal Motor Vehicle Safety Standards in the United States. The latter establish such requirements as: the windshield wiper system should not interfere with the driver's work but remain capable of cleaning the normatively defined area of the windshield during the specified number of cycles, etc. The UNECE R43 regulation also includes performance requirements for windscreen wipers and describes their ability to effectively clear the windscreen of dirt, rain, or snow. However, some para meters of these Rules need to be revised in order to comply with modern trends, for example control of the wiper pressure on the glass surface or the selection of alternative profiles of rubber brushes with an assessment of their effectiveness. Therefore, studies considering the development and optimization of the parameters of the working elements of windshield wipers in contact with the glass surface are relevant.

2. Literature review and problem statement

The review in [1] reflects the evolution of the design of windshield wipers and washers from 1939 to 2021, highlighting the main innovations aimed at optimizing windshield cleaning and improving road safety. It notes the increased risk of accidents in adverse weather due to potential visibility problems caused by wiper and washer systems and offers suggestions for future research areas to further improve these systems. At the same time, in the cited review there are no studies on alternative designs of wiper blades. Windshield wipers are primarily designed to remove water and dirt from the windshield [2], providing the driver with a clear view of the road ahead. Determining the efficiency of windshield wipers from the very beginning of their design is critically important for ensuring their reliable operation, which is the subject of numerous scientific works. Paper [3] investigates how variations in the curvature of the windshield affect the distribution of forces acting on the side of the windshield wiper and demonstrates the influence on the corresponding dynamics of transient processes. The study includes contact calculations for three different types of windshield curvature and three force application points in a finite element analysis (FEA) module. These data are further analyzed using a series of interconnected mass-spring damping systems to model the dynamic behavior of the wiper blade rib. Works [2, 3] do not contain studies of windshield wipers in critical operating conditions, which is one of the tasks of this work. Paper [4] delves into the complex non-linear interaction between the wiper blade and the vehicle glass using FEA, demonstrating how the shape of the brush affects the load distribution. Since the contact of the blade with the windshield depends on the movement of the windshield wiper, it is useful to refer to study [5], which focuses on the geometric synthesis of the mechanism of the front windshield wiper using rockers for fixing the brush. Wiper mechanisms are also studied in [6]. Despite the relevance of the topics addressed in [4–6], the authors do not provide data on the resulting pressure on the glass surface from the side of the windshield wiper. In [7], the dynamic characteristics and mechanism of generating vibrations of a frameless windshield wiper are studied. A wiper prediction scheme is proposed using a sectional linkage model to estimate vibrations caused by frameless structures and provides a detailed analysis of nonlinear dynamics. Work [8] investigates the dynamics of friction and vibrations during the interaction between a windshield wiper and a vehicle windshield by developing and testing dynamic and frictional models under various conditions. The aim is to provide a theoretical basis for the structural optimization of rubber blades. The authors of [7, 8] do not provide the results of a comparison of traditional and frameless windshield wipers, which is especially valuable from the point of view of friction and vibrations. In [9], the dynamics of wiper blades on a curved windshield were analyzed and attention was focused on such a parameter as the angle of attack, which contributes to the development of the problem of jumps. A two-link analytical model is introduced to study the interaction of dynamic and static friction using a variable gap control method to accurately determine the timing and conditions of transients affecting the jump phenomenon. Work [10] investigates the vibrations of front windshield wipers and their impact on driving comfort and safety by measuring contact forces at different points along the blade of the brush. The results show higher force and vibration values in the inner and middle sections of the blade, highlighting areas for targeted improvement in future research. Works [9, 10] consider the angle of inclination of the glass, but do not provide data on the effect of changing the radius of curvature of the glass on the obtained reactions and pressure distribution. In reality, the increase in the curvature of the glass helps reduce the load on the wiper at the edges – the uniformity of its fit deteriorates.

Considering the scientific novelty of the proposed double-row blade model, it is recommended to familiarize yourself with other novelties in the field of windshield wipers. Paper [11] presents an automatic wiper rain tracking system aimed at improving driver safety by using water sensors, an Arduino Uno, a servo drive, and an external power supply. Such a complex makes it possible to detect the intensity of precipitation and provide automatic control of the speed of the windshield wiper (in order to reduce mechanical errors and driver distractions). The authors of [12] also presented their automatic car windshield wiper system designed to minimize driver distraction by adjusting the windshield wiper speed according to the intensity of the rain and providing an audio signal about the downpour. The system consists of a rain sensor and a servo drive interacting with an ATMega328 (Arduino Uno A000066), showing fast responses and efficient operation, thereby increasing driving safety and potentially integrating with modern automotive technology. Automatic rain-sensing wipers using Arduino are the subject of [13]. Automotive engineers present precise mathematical formulas, applied to a three-dimensional elastic model with specific boundary conditions, to predict the vibration frequencies of the windshield wiper rubber brush [14]. This noise reduction model has been validated with experimental data, showing near-perfect fit, and providing a reliable tool for testing and improving wiper design. Papers [11–14] are based on Arduino but remain isolated from the vehicle user interface. Modern trends in control and driver interaction with car systems are often based on Android Automotive. Such a platform can effectively complement the sensors proposed by the authors, informing the driver about the intensity of rain and other parameters.

Despite the fact that the object of research is a conventional windshield wiper, it makes sense to get acquainted with the features of the geometric curvature of a frameless windshield wiper [15], which has nonlinear variable characteristics. Study [16] highlights a method for optimizing the geometry of metal flexible elements in flat windshield wipers by measuring the pressure distribution using piezoelectric sensors and using computer aided design (CAD) and FEA. The authors apply these techniques to curved windshields, perform dynamic wiping simulations, and compare practical cleaning performance with real-world numerical results to ensure optimal wiper performance. In works [15, 16] there is a lack of results comparing the pressure distribution from traditional and frameless wipers on the curved glass surface under the same boundary conditions. The topic of pressure on the glass surface was previously discussed in [17] – the intermediate state of the system under the action of a vertical load of 20 N applied to the windshield wiper frame was considered. The results showed that the load can be increased, taking into account the permissible limits of movement of the wiper blade according to the Rules R43 (1.5 mm), and therefore the studies are not exhaustive.

Paper [18] details the integration of CFD to evaluate the washoff performance of rainwater and windshield wiper fluid on automotive glass surfaces. The study determines the movement of the wiper blades based on Multi-Body Dynamics (MBD), taking into account variables such as the speed and range of the driver and passenger side wipers. The CFD theme continues in [19] – the authors of the study focus on evaluating the waterproof performance of vehicle windshield wiper systems using CFD software PreonLab to simulate water flows, thereby identifying areas of potential waterproofing failure. Study [20] uses numerical simulations to analyze the aerodynamic forces acting on windshield wiper systems at critical angles, focusing on blade geometry and spoiler modifications to counteract lift forces at high speeds. Optimum modifications such as wiper profile, height, and connection type are determined to minimize aerodynamic lift. The effectiveness of these changes has been confirmed through wind tunnel testing, proving that the new wiper design is more efficient and provides higher wiping performance. Despite the use of CFD, papers [18–20] are focused on the aerodynamics of windshield wipers, but do not provide data on hydrodynamics under various boundary conditions. The authors in works [21–23] seek to deepen the understanding of the transient aerodynamic effects of moving windshield wipers, using vortex simulation and dynamic grid methods to study the factors affecting the air flow and various aerodynamic forces. These works do not cover meteorological factors affecting the aerodynamics of the windshield wiper, for example, rain waves. An increase in the density of the environment leads to an increase in its resistance – aerodynamic indicators during rain differ from those in dry weather. The theoretical foundations of transient mechanical processes in Ansys Transient Structural are also described in [24] by the authors of this work. The work serves more as a theoretical reminder of the Ansys strength calculation principles applied in current research.

The research area of windshield wipers is quite popular among available scientific publications, however, there is a lack of modern works that consider the simulation of extreme conditions of operation of windshield wipers. The last fact is closely related to the modern trends of reducing budgets and deadlines for the development and testing of windshield wipers. The so-called “key performance indicators” (KPIs) at all levels of enterprise or laboratory activity dictated by austerity and market competition have additional influence. Extreme conditions of operation of windshield wipers may be the subject of attention of manufacturers of special or military equipment, information about which is limited to open publications. Such specific conditions include, for example, the investigated case of frozen rocker arms and immobilized windshield wiper frame. There is also relatively little research on new types of rubber wiper blade profiles. CFD analysis is an innovative direction since most scientists consider the aerodynamics of the wiper as a whole, rather than the hydrodynamics of an individual rubber blade. Therefore, the above studies show that the UNECE Regulations need to be updated to meet the current trends in the automotive industry.

3. The aim and objectives of the study

The purpose of our study is to determine the regularities of the mechanical and hydrodynamic parameters of the contact interaction of a two-row rubber wiper with a curved glass surface. This will make it possible to build analytical models for testing windshield wipers under extreme conditions and provide practical recommendations for designing a working prototype of a double-row rubber blade with individual brushes.

To achieve the goal, the following tasks were set:

– to investigate the parameters of the mechanical interaction of the windshield wiper with the surface of the windshield;

– to analyze the hydrodynamic contact of a double-row rubber blade with a curved glass surface.

4. Research materials and methods

4. 1. Interaction of the windshield wiper with a curved windshield

Below are the design features of a conventional windshield wiper based on a simplified assembly (Fig. 1) before conducting Ansys tests. A typical assembly structure of a conventional windshield wiper includes a retainer (1), a frame of the windshield wiper (2), a rubber brush with a blade (3), which together rotate on the axis of the drive bracket (4) and are pressed by a spring (5).

The spring (5) creates a load, which in the form of pressure is distributed over the surface of the glass with the help of the rubber blade of the brush (3). At the same time, the force distribution along the contact line cannot be assumed to be uniform. The frame (2) consists of movable links (rocker arms) that rotate on the respective axes (dashed lines in Fig. 1) to ensure full adherence of the blade to the glass surface. The rubber brush is clamped by rockers, usually at 8 points (marked by triangles in Fig. 1), through which concentrated forces are created on the rubber blade. It is impossible to compensate for the point load by selecting the appropriate stiffness of the wiper rubber brush, as this parameter is provided by the R43 Rules. The check can be performed by moving a brush over the surface of a standard container with a width of 80 mm or using other legally acceptable equipment. The main transverse dimensions of the rubber brush (visualized solid model in Fig. 2) are: the thickness of the blade (7) is 0.6 mm; the height of the blade (1) and the rest of the brush (3) is 5 mm each; neck (2) – 0.5 mm. Index numbers and values are taken from R43.

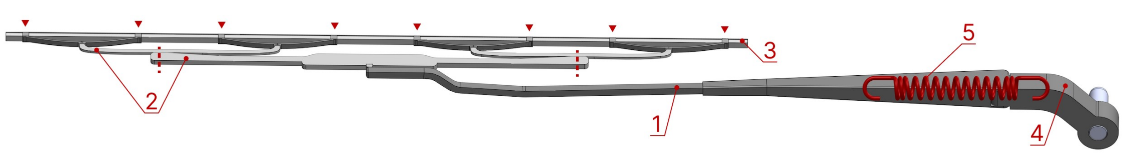

Fig. 1. Typical diagram of a regular windshield wiper model: 1 – retainer; 2 – frame; 3 – brush; 4 – bracket; 5 – spring

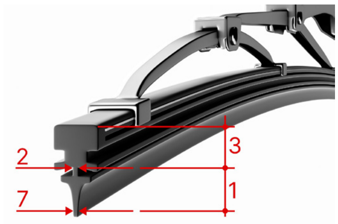

Fig. 2. R43 parameters of the cross-section of the wiper brush: 1 — 5 mm; 2 — 0.5 mm; 3 — 5 mm; 7 — 0.6 mm

Mathematical modeling of the interaction of the wiper with the glass surface (Fig. 3) can be carried out on the basis of Winkler's modified solution (model *a* in Fig. 3) – a linear elastic model. In the general case, it is a beam of infinite length x with width B and variable bending stiffness $EI(x)$ with an external load diagram $Q(x)$ and a single stiffness parameter k (1):

$$\sum_{i=1}^{m} P_i \delta(x-x_i) = Q(x) =$$
$$= EI(x)\frac{d^4 w(x)}{dx^4} + \frac{M(x)}{R_a^2}\frac{d^2 w(x)}{dx^2} + k \cdot B \cdot w(x), \qquad (1)$$

where P_i is the point load from the wiper rockers on the rubber blade (in this case, i=8, which corresponds to the triangles in Fig. 1); $\delta(x-x_i)$ is the Dirac delta function, and x_i is the location of the concentrated load (the load factor of the windshield wiper rockers); $w(x)$ is the vertical deflection of the beam, m; $M(x)$ is the moment along the beam caused by the curvature of the glass, Nm; R_a – radius of glass curvature, m; $EI(x)=E(x)\cdot I(x)$ – variable stiffness of the Euler-Bernoulli beam, Pa·m^4; B – beam width, m; k – hardness parameter (subgrade modulus), N/m^3.

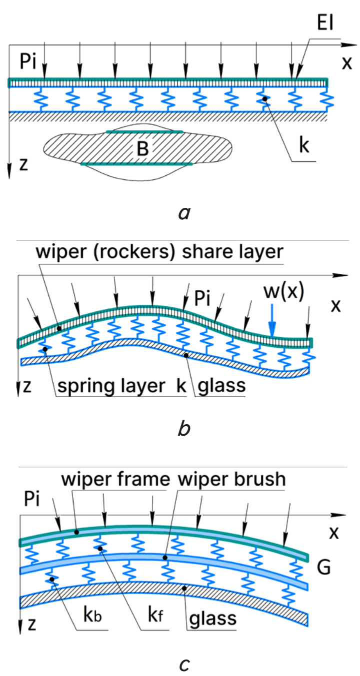

Fig. 3. Mathematical multilayer models: *a* — Winkler; *b* — Parsnip; *c* — Kerr

$E(x)$ represents the change in modulus of elasticity along the arc length x, which may include effects such as increasing or decreasing stiffness, etc. $I(s)$ is responsible for the change in moment of inertia along x, which takes into account modifications of the cross-sectional area of the brush blade due to the curvature of the contact surface of the wiper. The rubber brush receives different stresses along its length (will be confirmed in the results of the work), taking into account the unevenness of its adhesion to the glass. Then $I(x)$ for a blade with cross section $B\times h$ can be written as $B(x)h(x)^3/12$.

Winkler's approach takes into account the stiffness of the frame of the windshield wiper with rockers, and not their interaction during the shift, so it is advisable to refer to the Pasternak model (2) based on the modified Winkler model (1) (model *b* in Fig. 3):

$$\sum_{i=1}^{m} P_i \delta(x-x_i) = Q(x) = Wi(x) + L(w), \qquad (2)$$

where $Wi(x)$ are terms of the equation of the Winkler model (1); $L(w)$ is an operator that takes into account interactions during shear.

The surface of the glass and wipers are not rectilinear, which was demonstrated in model *b* (Fig. 3) and described in the modified Winkler model (radius of curvature R_a). In real cars, even $R_a \neq$const (curvature is not constant). If we denote the curvature of the surface by the function of the position along the beam $k(x)$, which takes into account the influence of curvature on stiffness, then the Pasternak model (2) will take the following form:

$$EI\left(\frac{d^4 w(x)}{dx^4} - 2k(x)\frac{d^2 w(x)}{dx^2} + 2k(x)^2 w(x)\right) +$$
$$+ L(w) + k \cdot B \cdot w(x) = Q(x). \qquad (3)$$

The specified transient process with the functions $k(x)$ and $w(x)$ (3) cannot be mathematically described by a discrete state, and therefore it is necessary to resort to such packages as Transient Structural (Ansys), which are able to calculate the intermediate positions of the system. We shall present other alternative mathematical models, for example, the Filonenko-Borodich model – the continuity of individual spring elements in the Winkler model with their connection in thin elastic membranes under tension T. The Hetenyi model – an elastic beam that is subjected to only bending deformations and applies the bending stiffness D of the elastic state. The elastic-plastic model (Rhines, 1969) and the Kerr model (Kerr – model *c* in Fig. 3), which is of greatest interest to us. This is due to the fact that a regular windshield wiper actually consists of two elastic layers: a frame with rockers and a rubber brush with a blade. Thus, the wiper pressure p_w on the glass surface can be found from the differential equation of the Kerr model in the following form (4):

$$p_w = \frac{k_b w(x) + \dfrac{G\nabla^2 p}{k_f} - G\nabla^2 w(x)}{1 + \dfrac{k_b}{k_f}}, \qquad (4)$$

where k_f is the elasticity of the frame layer (wiper with rockers); k_b – brush layer constant; G – shear modulus, Pa; $w(x)$ is the deflection of the framework layer (given that the deflection of the brush is relatively smaller, its value can be neglected, although this is an open topic for possible further research), m; ∇^2 is the Laplace operator.

Analysis was carried out for the most difficult case of wiper operation, when the surface of the windshield was curved, and the rubber blade had a straight profile. This is possible when the moving links (rockers) of the frame of the windshield wiper are frozen or acidified and blocked (do not rotate on the corresponding axes). Then the entire structure is immobilized, which often happens in winter, off-road, or due to the age of the car. The following boundary conditions were set in the Ansys Transient Structural module (Fig. 4):

– rigid fixation of the "Fixed Support" of the curved lower surface of the windshield (label C);

– zero displacement "Displacement" (label A) of the windshield wiper frame along the *Z* axis (parallel to the glass surface) throughout the experiment (duration=1 s with 5 steps of 0.2 s);

– force "Force" (label B) from the spring (element 5 in Fig. 1) applied to the center of the windshield wiper frame along the *Y* axis (perpendicular to the glass surface) with a modulus of 24 N. This value is the iteration of previous studies [17], the results which are not exhaustive from the point of view of the margin for the maximum permissible movements of the blade (1.5 mm according to R43);

– the length of the rubber blade is 0.5 m, and the coefficient of friction is 0.1;

– "Common glass", "Neoprene Rubber", and "Structural Steel NL" materials with a non-linear stressed-strained curve;

– FE-mesh of the model consists of 14268 elements and 41913 nodes.

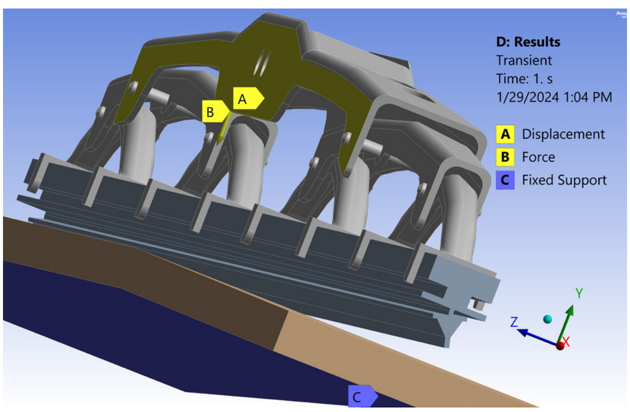

Fig. 4. Wiper boundary conditions in Ansys Transient Structural

4. 2. CFD analysis of the profile of the innovative rubber blade

The idea of our technological advancement refers to the "eternal" question: why do manufacturers of shaving machines equip them with several blades? Why does this not happen in the case of windshield wipers, which also have blades, but rubber ones? The built SolidWorks model (model *a* in Fig. 5) is a hybrid of a classic continuous rubber blade with an additional row of individual micro brushes located at an angle. Preliminary expectations of efficiency are based on the idea that each such brush acts like a broom, sweeping dirt from the glass surface on one side and passing streams of water through the channels on the other. Let's test the latter hypothesis by simulating it in the Ansys Fluid Flow module but before that, let's familiarize ourselves with the mathematical modeling approach and the theory of computation. The windshield wiper washes the volume of water V_w during one revolution t_{rot} (model *b* in Fig. 5) but the flow rate Q_w will additionally depend on k_d – the coefficient of dynamism, because in the same time t_{rot} the car travels a distance d_v. In fact, k_d determines how many times V_w must be considered during t_{rot}. The parameter V_w itself is the area of the water sector A_w multiplied by the height of the water layer H_{rot} according to the rain intensity *I*.

The first theoretical approximation of the calculation model Q_w (model *b* in Fig. 5) can be written in the form (5):

$$Q_w = \frac{V_w}{t_{rot}} k_d = \frac{A_w H_{rot}}{t_{rot}} \frac{d_v}{L_w \cos\alpha} =$$
$$= \frac{\left(\frac{\theta}{2}\left(R^2 - r^2\right)\right)\left(I \cdot t_{rot}\right)}{t_{rot}} \left(\frac{v_v \cdot t_{rot}}{L_w \cos\alpha}\right) =$$
$$= \frac{\theta \cdot I \cdot v_v \cdot t_{rot}\left(R^2 - r^2\right)}{2 L_w \cos\alpha}, \qquad (5)$$

where Q_w – water flow rate, m^3/s; V_w – the volume of rainwater falling on the windshield sector, formed by the rotation of the windshield wiper, m^3; k_d – coefficient of dynamism; A_w – sector area under V_w, m^2; H_{rot} – height of the rainwater sector, m; *I* – rain intensity, m/s; *R*, *r* are the outer and inner radii of the sector, m; θ – sector angle, rad; L_w – length of the wiper rubber brush, m; t_{rot} – time of 1 rotation (pass) of the windshield wiper, s; d_v – displacement of the car during t_{rot}, m; v_v – vehicle speed, m/s; α – angle of inclination of the windshield, °.

Taking into account the variability of the speed of the vehicle v_v and the intensity of rain *I* during the time t_{rot} (5), it is advisable to switch to the integral form of equation (6):

$$Q_w = \frac{\theta\left(R^2 - r^2\right)}{2 L_w \cos\alpha} \int_0^{t_{rot}} I(t) v_v(t) \mathrm{d}t. \qquad (6)$$

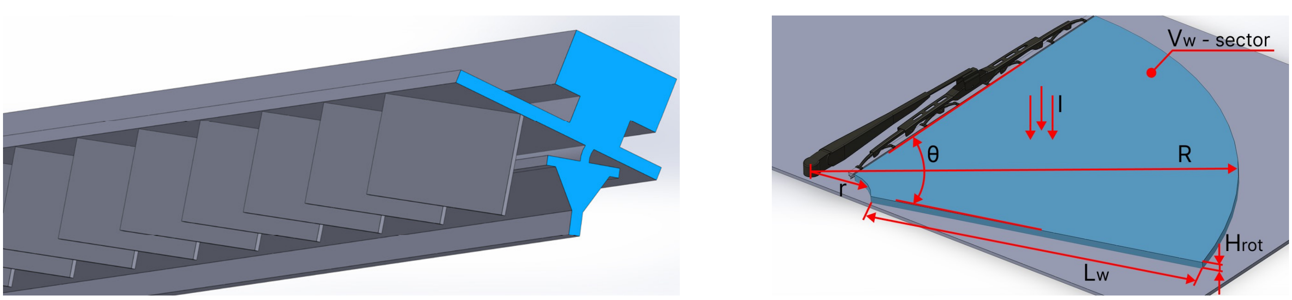

a *b*

Fig. 5. Simulating the modified windshield wiper brush: *a* — solid model with an additional row of individual brushes located at an angle; *b* — boundary conditions of the volume of the water sector

After determining the water flow rate Q_w (6), which the wiper must remove in 1 pass during t_{rot}, we proceed to the next step – calculating the speed of water passing the profile of the rubber blade. As you know, for a round pipe where the liquid moves laminarly (in layers without turbulence), the Hagen-Poiseuille equation can be applied for a cross section with a complex configuration and a variable area along the flow axis (7):

$$v_{HP}=\frac{1}{A_{HP}}\int\frac{Q_w}{\rho}\mathrm{d}A_{HP}, \qquad (7)$$

where v_{HP} is the velocity according to the Hagen-Poiseuille equation, m^2/s; A_{HP} is cross-sectional area, m^2.

More common is the Navier-Stokes equation, which is the basis of hydrodynamics, describing the movement of a liquid in three-dimensional space. Considering (6), for an unsteady fluid flow, the determination of the velocity v_f along the windshield wiper brush (x-axis) according to the Navier-Stokes equation (8) can be written as follows:

$$\mu\frac{\partial^2 v_f}{\partial x^2}=-\frac{\partial P}{\partial x},\ \text{or}\ \frac{\eta}{\rho}\cdot\frac{\partial^2}{\partial x^2}\cdot\frac{Q_w}{A(x,t)}=-\frac{\partial P}{\partial x}, \qquad (8)$$

where μ is kinematic viscosity, m^2/s; v_f – liquid flow rate, m/s; x – coordinate along the x axis, m; P – liquid pressure, Pa; ρ – liquid density, kg/m^3; η – dynamic viscosity, Pa·s; $A(x,t)$ – cross-sectional area, m^2.

When solving equation (8), several interrelated problems arose: $A(x,t)$ is a variable not only with respect to time t (the cross-sectional area of the water flow along the windshield wiper) but also with respect to the x coordinate, which greatly complicates the solution of this equation. In addition, under real conditions, the movement of water is not unidirectional, which increases the degree of complexity of differentiation with respect to all axes x, y, z (model *a* in Fig. 6). Thus, it seems appropriate to proceed to the CFD modeling of the water flow (model *a* in Fig. 6), which passes by the innovative wiper blade with separate brushes (model *a* in Fig. 5). The blue lines (model *a* in Fig. 6) correspond to the cross-sectional profile of the wiper blade, and the black lines correspond to the volume of water under it. To simplify the calculation, part of the length of the solid model of this volume of water was simulated (model *b* in Fig. 6).

Let's analyze the geometric parameters of the cross section of the water flow volume (model *a* in Fig. 6): $A_z \cong$const is a stable value determined by the physical height of the blade profile. It can fluctuate within very small limits (0.1–0.25 mm max) due to changes in the pressure of the windshield wiper on the glass, which was studied above in chapter 4.1. $A_y \neq$const is a variable parameter since the area $A(x,t)$ (8) depends on the rain intensity I, which was also demonstrated in (6). In fact, A_y is responsible for how much water the wiper washes in 1 pass.

In the Ansys Fluid Flow model (Fig. 7), the incoming water flow with a speed of v_i=0.5 m/s corresponds to the blue areas (face *a* in Fig. 7), and the outgoing water flow to the red (face *b* in Fig. 7) with the A_{outlet} area.

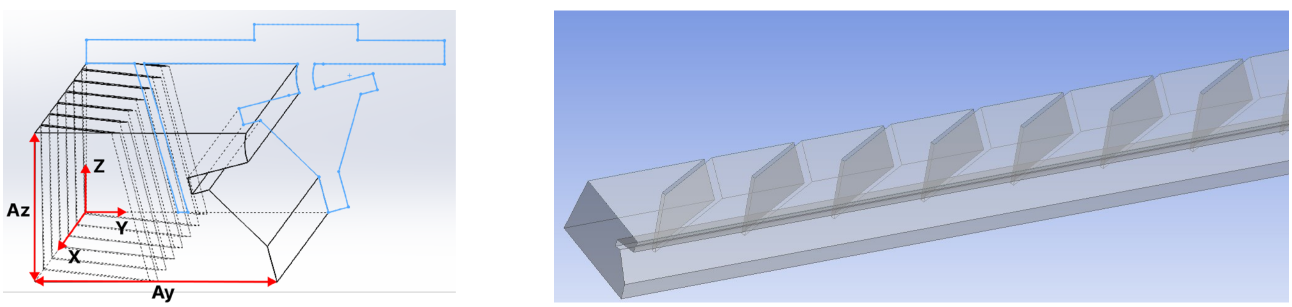

a *b*

Fig. 6. The volume of water passing by the modified wiper blade with brushes: *a* — cross section of the volume of water (black lines) under the blade (blue lines); *b* — part of the Ansys water volume model

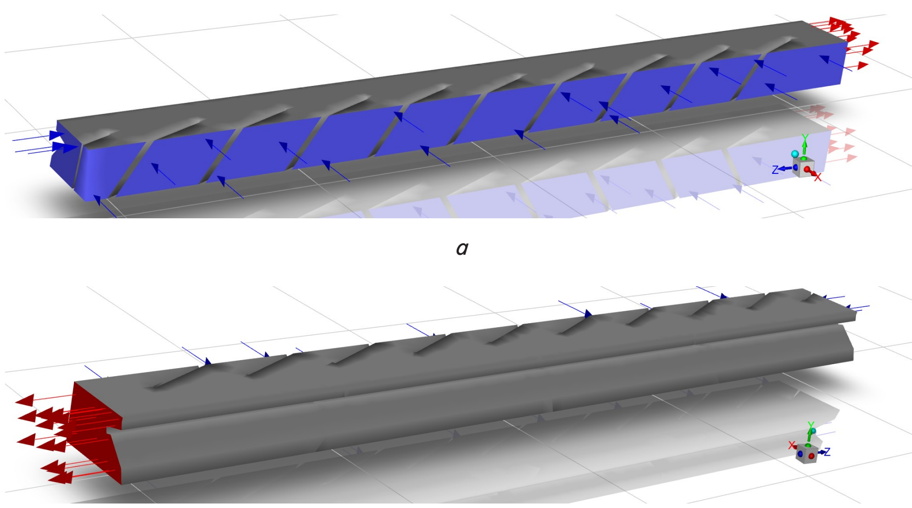

a

b

Fig. 7. Ansys Fluid Flow boundary conditions: *a* — input flow; *b* — output flow

Such boundary conditions already clearly demonstrate the fact of changing the parameter $A(x,t)$ (8) in time and coordinates. Boundary conditions of water: density, 998.2 kg/m^3; viscosity, 0.001003 kg/(m·s); the number of Ansys calculation iterations, 500; the ambient temperature, 22°.

5. Results of investigating the mechanical contact and hydrodynamic parameters of the double-row wiper

5. 1. Mechanical interaction of the windshield wiper with the windshield

Analysis of the stressed-strained state of the windshield wiper during contact with the curved glass has made it possible to establish the following results.

Modeling of the real operating conditions of the windshield wiper cannot be completely replaced by the above mathematical models, which is clearly visible in the unevenness of the complete movements of the rubber blade along its length (Fig. 8). Even Kerr's model (4), which is closest in terms of factors to imitation of natural behavior (4), is insufficient. It does not fully take into account the change in the stiffness of the windshield wiper along its length – in fact, the coefficients k_b and k_f should be functions. Thus, the calculated pressure on the surface (4) should be variable along the length of the windshield wiper, which we can observe from the results of the stressed-strained maps of the rubber blade. The Mieses stress values are 0.112 MPa and are recorded in the central part of the blade (map *a* in Fig. 8). The total displacements were 1.48 mm (map *b* in Fig. 8) at the ends of the blade, which, despite the noticeable deflection, did not reach contact with the glass.

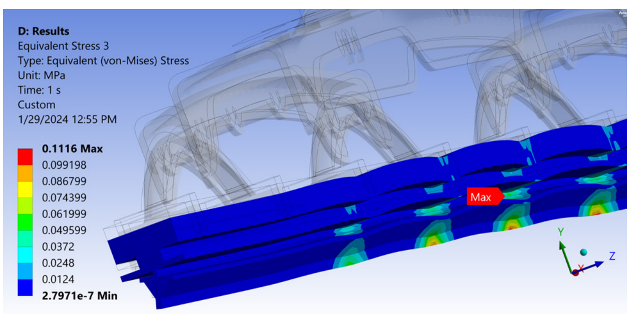

a

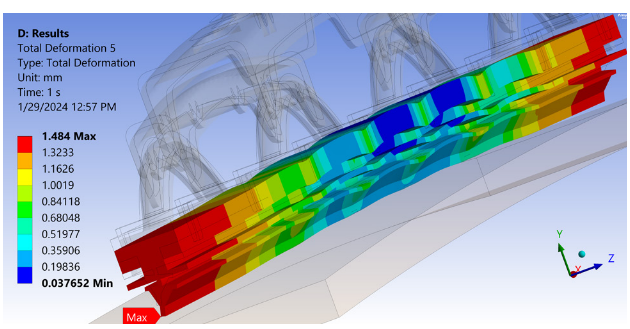

b

Fig. 8. Stressed-strained state of the windshield wiper: *a* — stress according to Mieses; *b* — total displacements

The Mieses stress map clearly shows the non-uniformity of the pressure distribution from the blade to the glass surface (the maximum value of 33.4 kPa is observed on map *a*, Fig. 9). The maximum Mieses stress for the entire model in general is 104.75 MPa and is observed on the axes of the wiper frame rockers (map *b* in Fig. 9). This is a fairly high value relative to the yield strength (124 MPa for brass). The location of these stresses is predictable since the established boundary conditions (Fig. 4) provided for the jamming of the indicated axes to simulate the most difficult case of operation.

Despite the linear growth of the external load on the frame (Fig. 4) during the experiment (1 s), the movement and deformation of the blade in the selected locations (model *a* in Fig. 10) are completely non-linear. This is clearly observed in plots *b*, *c* in Fig. 10.

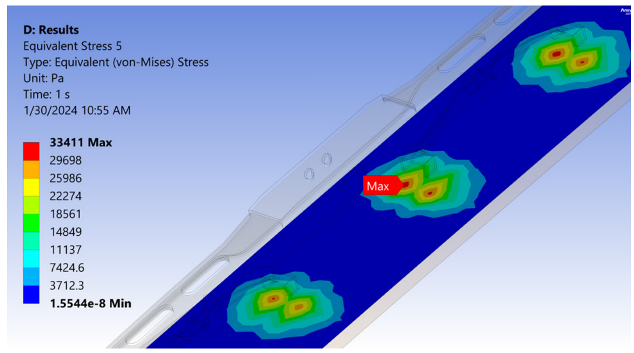

a

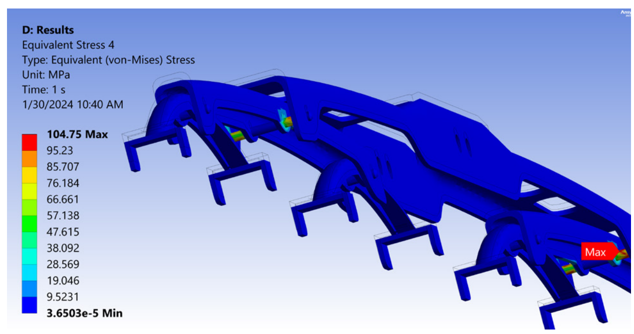

b

Fig. 9. Stress maps according to Mieses: *a* — glass surface; *b* — windshield wiper frame

In the process of further loading of the windshield wiper frame, plastic deformations can be observed precisely in the critical areas of the rubber brush. This is traced under each of the specified 8 rocker arm clamps (model *a* in Fig. 10), which correlates with mathematical modeling. Such zones are subjected to the load *Pi*, which is included in equations (1) to (3). The displacements increased to 1.82 mm (map *a* in Fig. 11), and the geometric shape locally has a "cut" character. Plastic deformations will certainly lead to the appearance of thin jets of dirt or water on the glass under real conditions due to the distortion of the shape of the blade (map *b* in Fig. 11). In some cases, the given local changes in the shape of the blade may become irreversible, which will require the driver to completely replace the wiper rubber brush.

An increase in the load also leads to global deformations – the loss of the shape of the rubber brush with its swelling in the space between the clamps and a lag of more than 5.7 mm from the glass surface. The large gap formed (map *c* in Fig. 11) between the blade and the glass will inevitably lead to the appearance of a blind zone and a significant deterioration of the driver's visibility, especially under severe weather conditions.

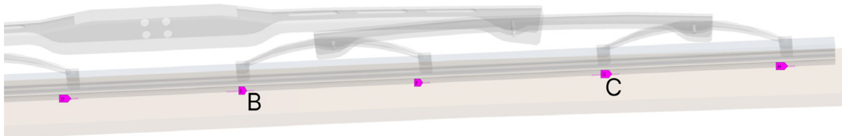

a

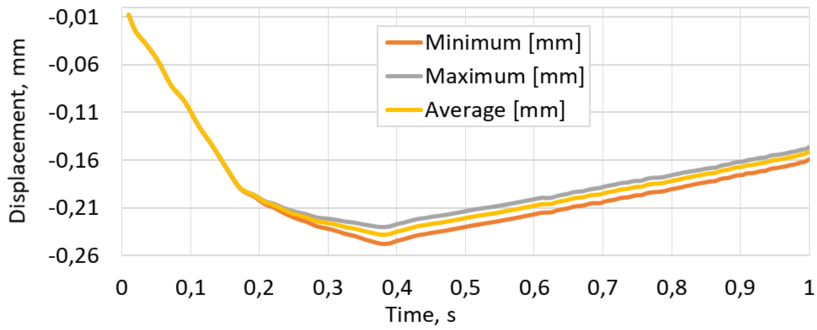

b

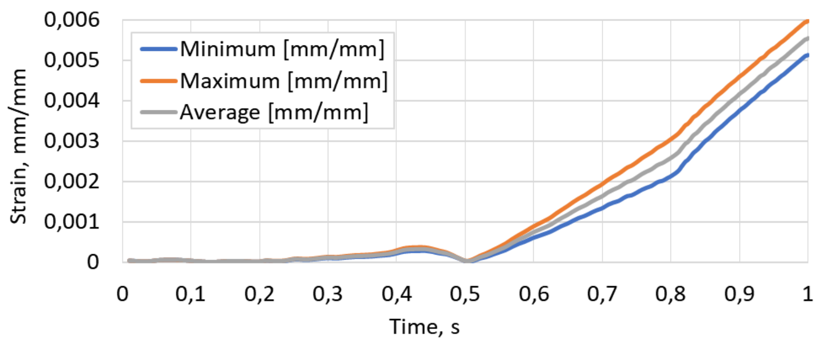

c

Fig. 10. Clamps with rockers: *a* — location points; *b* — displacement of point B; *c* — deformations of point C

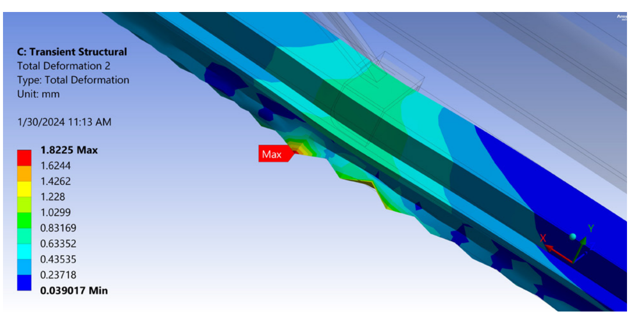

a

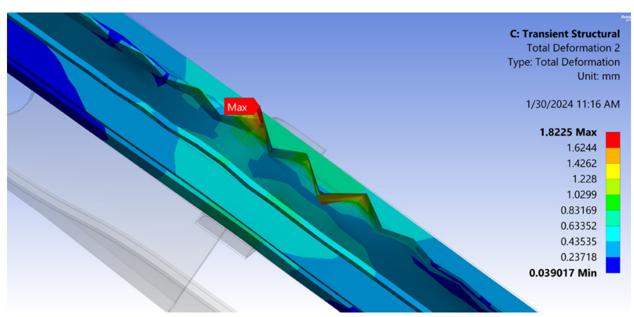

b

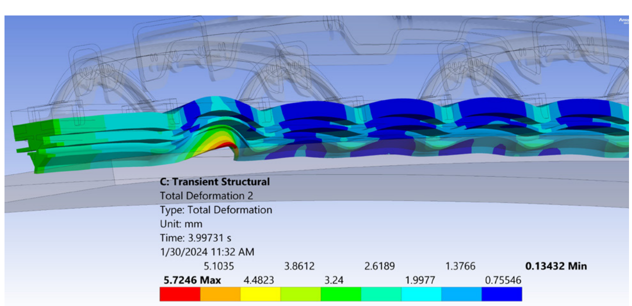

c

Fig. 11. Complete movements of the windshield wiper brush: *a*, *b* — local (general and bottom view); *c* — global (loss of shape)

5. 2. Results of the analysis of the hydrodynamic contact of a double-row rubber blade with a curved glass surface

Four calculation models were analyzed (Table 1): No. 1 – a classic brush with a single-row solid wiper blade and No. 2–4 – models with an additional row of individual brushes and a different range of the parameter A_y, which directly affects the area of the outlet channel A_{outlet}. The criterion for the efficiency of the windshield wiper brush was the maximum fixed speed of water flows v_{max}. Therefore, the faster the windshield wiper washed a given volume of water in 1 revolution, the less liquid and dirt remained on the glass surface.

Water flow simulations for different models in the Ansys Fluid Flow module allow us to visually compare the velocity results (Fig. 12).

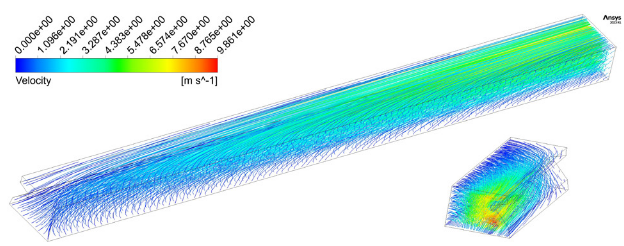

a

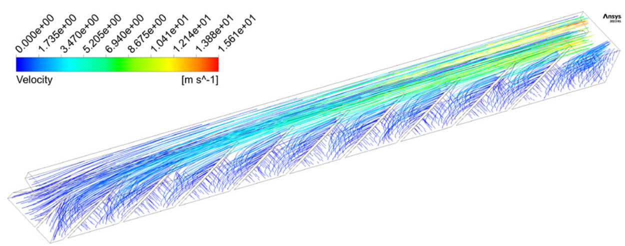

b

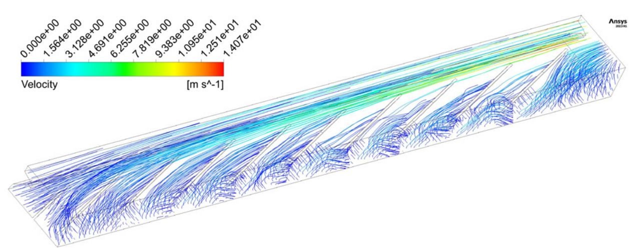

c

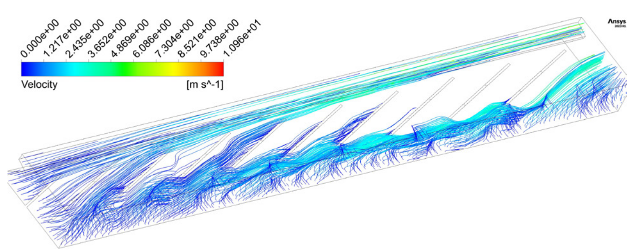

d

Fig. 12. Velocity results of Ansys Fluid Flow models: *a* – flat single row; *b* – #2; *c* – #3; *d* – #4

Despite the visual laminar speed demonstration shown in Fig. 12, in fact water flows are partially turbulent. This is clearly visible on the volumetric filling of model No. 3 (Fig. 13) – red clumps with local vortices (maximum values of velocity).

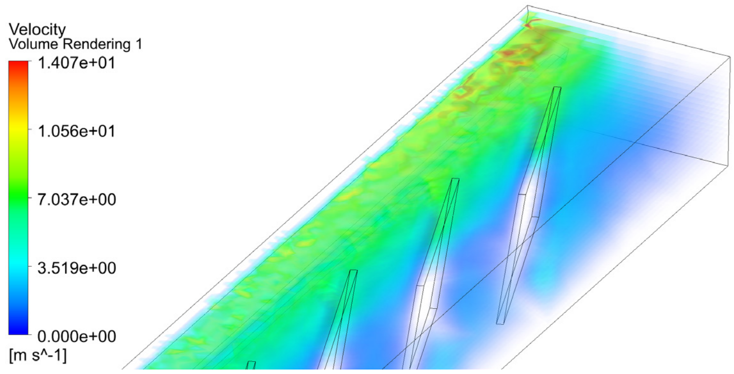

Fig. 13. Visualization of speed by volumetric filling of model No. 3

The distribution of the output velocity v_{outlet} along the outlet plane (red region *b* in Fig. 7) with the area A_{outlet} is shown in Fig. 14, and the values are indicated in Table 1.

Table 1

Dynamic characteristics of different wiper blade configurations in Ansys Fluid Flow

No.	Blade type	A_y, m	A_{outlet}, t^2	v_i, t/s	v_{max}, t/s	v_{outlet}, t/s
1	Flat blade	0.007	2.6244×10^{-5}	0.5	9.861	9.562
2	With brushes	0.007	2.6244×10^{-5}	0.5	15.61	15.14
3	With brushes	0.009	3.5041×10^{-5}	0.5	14.07	13.65
4	With brushes	0.011	4.3397×10^{-5}	0.5	10.01	9.703

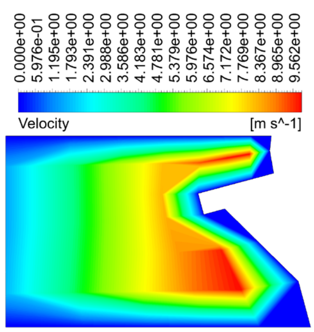

a

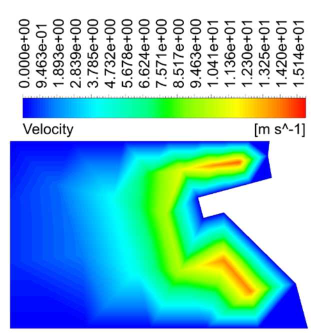

b

Fig. 14. Velocity maps on the outlet plane A_{outlet} of the blade model: *a* – flat; *b* – #2

From the given maps, it is possible to judge the distribution of velocities in the perpendicular plane of the windshield wiper and observe hydrodynamic trends.

6. Discussion of results of investigating the interaction between the windshield wiper and the glass surface and the hydrodynamics of the windshield wiper blade

Our research results, as well as those proposed by other authors [17], show that the optimal average value of the force of pressing the frame of the windshield wiper (2) by the spring (5 in Fig. 1) is »20 N. According to our results, it was established that the loads should not exceed 24 N for this wiper configuration. A lower load value may not ensure sufficient adhesion of the wiper to the glass at the edges of the rubber brush in extreme operating conditions. The rubber blade showed a total displacement of 1.48 mm in the central part (map *b* in Fig. 8), which is quite a high indicator. Judging by the R43 wiper blade regulatory requirements (Fig. 2), the maximum total movement cannot exceed 1.5 mm since the height of the neck 2 is only 1 mm. Thus, for the specified materials ("Neoprene Rubber" and "Structural Steel NL") and geometrical parameters of the windshield wiper, the load value of 24 N is the upper limit in the case of mechanical immobilization. The frozen state of the rockers leads to an increase in Mieses stresses in their axes up to 104.75 MPa (map *b* in Fig. 9), which is close to the yield point of brass (σ_m=124 MPa). The maximum value of pressure (33.4 kPa) was also recorded in the contact spots of the windshield (map *a* in Fig. 9), which correspond to the position of the rocker arms. This value is not critical but during accidental release of the spring-loaded wiper, it can increase several times and lead to impact on the glass and the appearance of cracks at low temperatures.

Further loading of the frame of the windshield wiper was accompanied by the appearance of deformations of two types: local and global (loss of the shape of the rubber brush). Local ones are manifested in the form of movements at the level of 1.82 mm (higher than the permissible 1.5 mm according to R43) and the appearance of thin jets of dirt or water on the glass as a result of cutting the blade. Global leads to the loss of the shape of the rubber brush with its swelling in the space between the clamps and the formation of a gap of 5.7 mm between the glass and the blade (map *c* in Fig. 11). This will certainly cause the appearance of a blind zone and a significant deterioration of the driver's visibility. Among modern passenger cars for masses, only the Mercedes-Benz G-Class and Tesla Cybertruck models have flat windshields, but on other cars the curvature and area of the glass is constantly increasing with each new generation. Our results of the distribution of pressure on stresses testify to the solution of the problem of studying the interaction of the windshield wiper with the curved surface of the glass. In contrast to [2–10], in which variants of the absolute repeatability of the curvature of the windshield wiper and the glass surface are considered, the current research data demonstrate the application of other possible cases of operation.

Among the considered mathematical models for calculating the distributed load, the Kerr model turned out to be the closest in compliance with the boundary conditions of full-scale tests compared to Winkler's or Pasternak's solutions. A conventional wiper actually consists of two elastic layers: a frame with rockers and a rubber profile with a blade, which correlates best with Kerr's approach. The problem is that such a transient process as the presented calculation case (an immobilized frame pressed against a curved windshield) with functions $k(x)$ and $w(x)$ cannot be mathematically described by a discrete state. It is impossible by mathematical modeling to achieve such local full displacements as 1.82 mm obtained using FEA in the Ansys Transient Structural module (Fig. 11). Actually, this point can be attributed to the so-called limitations and shortcomings of our study from the point of view of its application in practice. On the other hand, the proposed mathematical models could serve as a basis for further theoretical research, which is a subject of scientific value because this approach is less resource-intensive than FEA with its iterations.

The reviewed literature [2–10, 15–23] does not sufficiently describe other variants of rubber blades, except for the traditional single-row one. A variant of the rubber blade with an additional row of individual brushes located at an angle has shown useful practical results. With the same initial area A_{outlet}, the wiper blade with brushes No. 2 (Fig. 12) provided 1.58 times higher speed $v_{\max}$ than in the case of the classic single-row model No. 1 (15.61 vs. 9.861 m/s). And even with a 1.73-fold increase in water volume when going from No. 1 to No. 4, the velocity values are almost the same. This confirms the effectiveness of the design of the brushes of the second row, which are used in No. 4 (A_{outlet} in No. 1 is 2.6244 m^2 against 3.5041 m^2 in No. 4).

The proposed additional individual brushes act as turbine blades, creating additional centrifugal accelerations of water flows, which is clearly visible in the visualization of the volumetric filling of model No. 3 (Fig. 13). The distribution of the output velocity v_{outlet} along the outlet plane (red area of model *b* in Fig. 7) with the area A_{outlet} (Fig. 14) coincides with the trend of the volumetric analysis described for $v_{\max}$ (v_{outlet} is 15.14 m/s for model No. 2 against 9.562 m/s for No. 1). The following trend can be observed: the larger the value of A_y (model *a* in Fig. 6), the more distant water flows in the discharge plane (models *d* and *c* in Fig. 12, 14). Thus, a 2-row blade model is implemented – the first layer removes dirt, snow, and water with separate brushes, and the second one finally cleans the surface. Our results testify to the hydrodynamic analysis of the proposed innovative blade. Studies [18–23] that considered the CFD problem were focused on the flow of air currents around windshield wipers but did not investigate the hydrodynamics of windshield wiper blades. The limitations of our research on hydrodynamics are manifested in the coverage of possible combinations of sizes and angles of inclination of individual brushes, their distance from the main row and physical and mechanical properties of rubber. To carry out multifactor modeling, it may be necessary to build individual AI models for iterative prediction of optimal combinations of the specified parameters. The next step involves CFD verification of the results in the Ansys Fluid Flow module and the construction of a physical sample of the double-row blade, which requires financial costs for the production of the prototype.

Our research may be advanced toward selecting optimal configurations of rubber brushes for the second row: length and thickness, angles of inclination and distance from the main row, as well as rubber stiffness. The problems of combinatorics under conditions of multifactoriality belong to the obvious difficulties of the current research: field testing of physical samples is expensive while mathematical modeling is time-consuming and insufficiently accurate. Perhaps it is appropriate to involve AI with the construction of appropriate mathematical models for the iterative search for the optimal combination of indicators, both from the point of view of hydrodynamics and the uniformity of pressure distribution. This stage could be the next one, preceding the registration of a patent for a utility model or invention.

7. Conclusions

1. It was established that the pressure value should not exceed 30–50 kPa, and the external normal load on the frame of the windshield wiper by the spring should not exceed 20–30 N. The blade of a conventional windshield wiper was deformed by 1.48 mm under the action of a load of 24 N. According to Rules R43, the maximum value of the full movement cannot exceed 1.5 mm, therefore, for this wiper configuration, the applied load is the maximum allowable. Local pressure spots on the glass with a maximum Mieses stress value of 33.4 kPa were obtained, which decreased to zero at the ends of the windshield wiper, where a gap was formed. Such an uneven load distribution significantly reduces the area of windshield cleaning (to 40 %) and can create water drainage between the specified spots. Under the jamming mode of the rockers on their axes, the maximum Mieses stresses are formed at the level of 104.75 MPa, which is at the yield point of brass (124 MPa). Despite the linear growth of the load to a maximum of 24 N within 1 s, the magnitude of the complete movements of the rubber blade in the places of the clamps under the rockers (Fig. 10) is non-linear. Further loading of the wiper frame causes plastic deformations (local and global) in the vicinity of these clamps. The total displacements increased to 1.82 mm, and the geometric shape in this zone had a "cut" character (local deformations), creating thin jets of dirt on the surface of the glass (Fig. 11). Global deformations were manifested in the loss of the shape of the rubber brush and the formation of a gap between it and the glass (5.7 mm), which significantly worsens visibility in bad weather. None of the analyzed models (Winkler or Pasternak) can provide the magnitude of such plastic deformation, as it does not take into account transient processes.

2. We have proposed a structure of a double-row blade with separate brushes. With the same outlet area A_{outlet}, the model No. 2 wiper brush demonstrated 1.58 times higher speed $v_{\max}$ than classic single-row model No. 1 (15.61 vs. 9.86 m/s). The described design of the blade allows the passage of a much larger volume of water at the same time. With an almost two-fold increase in water volume between models No. 1 and No. 4, the velocity values remained almost the same, which confirms the effectiveness of brushes of model No. 4 (A_{outlet} in No. 1 is 2.6244 m^2 versus 3.5041 in No. 4). The output velocity distribution v_{outlet} matches the volumetric analysis trend described for $v_{\max}$. This means that the designed model of the blade is not inferior in efficiency at the final stage of releasing the consumed volume of water. The higher the value of A_y (ranging from 0.007 to 0.011 m – model *a* in Fig. 6), the more distant water flows in the outlet plane (model *d* in Fig. 12). At the same time, the speed of the external flow also increases (5.5–6.8 m/s for model No. 4).

Conflicts of interest

The authors declare that they have no conflicts of interest in relation to the current study, including financial, personal, authorship, or any other, that could affect the study and the results reported in this paper.

Funding

The study was conducted without financial support.

Data availability

All data are available in the main text of the manuscript.

Use of artificial intelligence

The authors confirm that they did not use artificial intelligence technologies when creating the current work.

References

1. Kaur, H., Nirmal, U. (2022). A Review on the Development of Wiper System for Automotive Car Windscreen Cleaning Application. Current Journal of Applied Science and Technology, 41 (7), 1–27. https://doi.org/10.9734/cjast/2022/v41i731675
2. Jhung, J., Kim, S. (2021). Behind-The-Scenes (BTS): Wiper-Occlusion Canceling for Advanced Driver Assistance Systems in Adverse Rain Environments. Sensors, 21 (23), 8081. https://doi.org/10.3390/s21238081
3. Graham, B., Knowles, J., Mavros, G. (2023). The influence of contact distribution shaping on the dynamic response of a wiper blade. Proceedings of the Institution of Mechanical Engineers, Part D: Journal of Automobile Engineering, 095440702311647. https://doi.org/10.1177/09544070231164792
4. Graham, B., Knowles, J., Mavros, G. (2023). Quantitative Multi-Physics Tools for Automotive Wiper Design. SAE Technical Paper Series. https://doi.org/10.4271/2023-01-0602
5. Antonescu, O., Valeanu, D., Antonescu, D., Strimbeanu, M. (2023). Contributions to the Geometric Synthesis of the Windshield Wiper Mechanism with Rocker-Slider Blade. Mechanisms and Machine Science, 404–413. https://doi.org/10.1007/978-3-031-45709-8_40
6. Sharveswaran, A., Nirmal, U. (2020). Research Development on Wiper Mechanism in Automotive Application: A Critical Review. Current Journal of Applied Science and Technology, 39 (35), 133–161. https://doi.org/10.9734/cjast/2020/v39i3531064
7. Li, Y., Xu, J. (2022). Dynamic characteristics and generation mechanism of windscreen frameless wiper blade oscillations. Nonlinear Dynamics, 111 (4), 3053–3079. https://doi.org/10.1007/s11071-022-08030-0
8. Yang, X., Wang, Y., Guo, H., Yuan, T., Zheng, L., Sun, P. (2022). A theoretical analysis of friction and vibration characteristics of wiper reversal process. Proceedings of the Institution of Mechanical Engineers, Part D: Journal of Automobile Engineering, 237 (6), 1327–1337. https://doi.org/10.1177/09544070221091021
9. Zhao, Z., Yabuno, H., Kamiyama, K. (2022). Dynamic Analysis of a Wiper Blade in Consideration of Attack Angle and Clarification of the Jumping Phenomenon. Applied Sciences, 12 (9), 4112. https://doi.org/10.3390/app12094112

10. Salleh, I., Z. Md Zain, M., R. Abu Bakar, A. (2018). Contact Force and Dynamic Behavior of Automobile Wiper Blade System. International Journal of Engineering & Technology, 7 (3.17), 100. https://doi.org/10.14419/ijet.v7i3.17.16630
11. Roland, A., Wejin, J., Misra, S., Sharma, M. M., Dama evi ius, R., Maskeli nas, R. (2022). A Dynamic Rain Detecting Car Wiper. Lecture Notes in Networks and Systems, 1375–1383. https://doi.org/10.1007/978-3-030-96308-8_127
12. Akanni, J., Ojo, A. O., Abdulwahab, A., Isa, A. A., Ogunbiyi, O. (2022). Development and Implementation of a Prototype Automatic Rain-Sensor Car Wiper System. Journal of Applied Sciences and Environmental Management, 26 (11), 1821–1826. https://doi.org/10.4314/jasem.v26i11.13
13. Yadav, S. (2021). Automatic Rain Sensing Wiper using Arduino. International Journal for Research in Applied Science and Engineering Technology, 9 (VI), 5434–5438. https://doi.org/10.22214/ijraset.2021.36065
14. Chen, T., Hong, Y. (2020). Mathematical Formulae for the Vibration Frequencies of Rubber Wiper on Windshield. arXiv. https://doi.org/10.48550/arXiv.2003.06022
15. Yunpeng, L., Jingjing, X., Xin, W. (2021). Shape analysis and numerical fitting of boneless wiper reed. Journal of Physics: Conference Series, 1939 (1), 012049. https://doi.org/10.1088/1742-6596/1939/1/012049
16. Huang, T. C., Tsai, J. W., Liao, K. C. (2021). Geometry Optimization of a Metallic Flexor for Flat Wipers. International Journal of Automotive Technology, 22 (3), 823–830. https://doi.org/10.1007/s12239-021-0075-6
17. Holenko, K., Voichyshyn, Y., Svidersky, V., Klypko, O. (2023). Simulation of wiper behavior during contact with a curved surface, factors affecting driving safety. Advances in mechanical engineering and transport, 1 (20), 127–137. https://doi.org/10.36910/automash.v1i20.1041
18. Shirsikar, A., Khatik, P., Singh, K., Ram, L. (2022). Optimized Wiper Design using Computational Fluid Dynamics. ARAI Journal of Mobility Technology, 2 (4), 401–410. https://doi.org/10.37285/ajmt.2.4.8
19. Yan, J., Zhu, K., Huang, X., Chen, K. (2022). Design Modification of Vehicle Body Structure for Wiper System Waterproof Performance. Proceedings of China SAE Congress 2021: Selected Papers, 1093–1102. https://doi.org/10.1007/978-981-19-3842-9_85
20. Dykha, A., Makovkin, O. (2019). Physical basis of contact mechanics of surfaces. Journal of Physics: Conference Series, 1172, 012003. https://doi.org/10.1088/1742-6596/1172/1/012003
21. Chen, Z., Gu, Z., Jiang, T. (2019). Research on transient aerodynamic characteristics of windshield wipers of vehicles. International Journal of Numerical Methods for Heat & Fluid Flow, 29 (8), 2870–2884. https://doi.org/10.1108/hff-09-2018-0531
22. Marchenko, D., Dykha, A., Aulin, V., Matvyeyeva, K., Tishechkina, K., Kurepin, V. (2020). Development of Technology and Research of Method of Electric Hydropulse Hardening of Machine Parts. 2020 IEEE Problems of Automated Electrodrive. Theory and Practice (PAEP). https://doi.org/10.1109/paep49887.2020.9240796
23. Cadirci, S., Ak, E. S., Selenbas, B., Gunes, H. (2017). Numerical and Experimental Investigation of Wiper System Performance at High Speeds. Journal of Applied Fluid Mechanics, 10 (3), 861–870. https://doi.org/10.18869/acadpub.jafm.73.240.26527
24. Holenko, K., Koda, E., Kernytskyy, I., Babak, O., Horbay, O., Popovych, V. et al. (2023). Evaluation of Accelerator Pedal Strength under Critical Loads Using the Finite Element Method. Applied Sciences, 13 (11), 6684. https://doi.org/10.3390/app13116684